Piperazine Analog of Vesamicol: In Vitro and In Vivo Characterization for Vesicular Acetylcholine Transporter

KAZUNORI BANDO,[1]* TOMOYOSHI NAGANUMA,[1] KAZUMI TAGUCHI,[1] YASUSHI GINOZA,[1] YOSHITOMO TANAKA,[1] KATSUO KOIKE,[2] AND KEIZO TAKATOKU[1]
[1]*Research Center, Daiichi Radioisotope Laboratories, Ltd., Chiba, Japan*
[2]*Department of Chemical Pharmacology, Toho University School of Pharmaceutical Sciences, Chiba, Japan*

KEY WORDS autoradiography; cholinergic; radioiodinated ligand; synaptic vesicle; vesamicol

ABSTRACT The probes to detect vesicular acetylcholine transporter (VAChT) in vivo are important to evaluate the mapping and function in cholinergic system. To develop high-specific and high-affinity radiotracer for single photon emission computed tomography, we investigated piperazine analogs which replaced the piperidine ring of (-)-vesamicol with a piperazine ring. We found that the piperazine analog of iodobenzovesamicol, trans-5-iodo-2-hydroxy-3-[4-phenylpiperazinyl] tetralin (DRC140), had high affinity for VAChT in rat brain. We carried out binding assay in subcellular fraction of the rat brain. The highest B_{max} for [^{125}I]-DRC140 binding was observed in the synaptic vesicle fraction (1,751 fmol/mg protein), followed by the crude vesicle (821 fmol/mg protein) and the P2 fraction (187 fmol/mg protein). These K_d values were similar to the affinity of highly purified synaptic vesicular fraction (K_d = 0.3 nM) with a one-site model. The possibility that [^{125}I]-DRC140 recognizes sigma receptor was excluded by our finding large inhibition constants (K_i = 849 nM for haloperidol, K_i = 3,052 nM for 1,3-di(2-tolyl)guanidine). In vivo distribution studies with the [^{123}I]-DRC140 in rats showed a rapid brain uptake. The highest brain area was in striatum, followed by frontal cortex, occipital cortex, and hippocampus. The lowest brain area was cerebellum. The radioactivity of high-accumulated areas in ex vivo autoradiography was reduced by a preinjection of (-)-vesamicol and these levels were reduced to the radioactivity in cerebellum. These results show that [^{125}I]-DRC140 can provide extremely high specific tracer with excellent brain permeability as a ligand for single photon emission computed tomography. **Synapse 38:27–37, 2000.**

INTRODUCTION

Alzheimer disease (AD) is known to be associated with a dramatic loss of acetylcholine and its related enzymes. The data from biopsy and autopsy samples from the brain of AD suggest that deficiencies of choline acetyltransferase (ChAT), high-affinity choline transporter, and acetylcholine esterase are initial neurochemical changes (Davies and Maloney, 1976; Perry et al., 1978, 1980; Wilcock et al., 1982). The vesicular acetylcholine transporter (VAChT) was located in the small synaptic vesicle, which accumulates acetylcholine synthesized in cytoplasm and releases it by exocytosis in cholinergic neurons. The detection of VAChT provides a unique tool for studying the function of cholinergic neurons in AD brain. The VAChT gene has been cloned from *Caenorhabditis elegans*, *Torpedo*, rat, and human (Alfonso et al., 1993; Varoqui et al., 1994; Erickson et al., 1994; Roghani et al., 1994). Interestingly, the coding sequence for VAChT is located completely within the first intron of ChAT gene in all species examined (Usdin et al., 1995). On account of these two proteins colocalizing in cholinergic neurons, there may be a common regulatory mechanism and coordinate transcription of the two genes. However, initial pharmacological studies of [^{3}H]-vesamicol binding in postmortem AD brain showed that binding site of the tracer was only slightly reduced as compared with the controls in frontal cortex (Kish et al., 1990) and increased significantly with the severity of dementia in temporal cortex (Ruberg et al., 1990). In an animal experiment, [^{3}H]-vesamicol binding and ChAT

*Correspondence to: Kazunori Bando, Research Center, Daiichi Radioisotope Laboratories, Ltd., 453-1, Shimo-Okura, Matsuo-Machi, Sanbu-Gun, Chiba, Japan, 289-1592.

Received 18 August 1999; Accepted in revised form 17 December 1999

activity were reduced by approximately 30% and in hippocampus after transection of the fimbria and frontal cortex after lesions of the basalis magnocellularis. At this time, ChAT activity was reduced by 60% in hippocampus and 50% in frontal cortex, respectively (Marien et al., 1987; Altar and Marien, 1988). However, recent animal studies in which the septohippocampal pathway was lesioned by a fimbria-fornix lesion or an immunotoxin lesion indicated a decrease of VAChT protein, as well as ChAT activity and coordinately expression in cholinergic terminals and cell bodies (Gilmor et al., 1998).

One of the possible reasons for the apparent discrepancy is low specificity of [^{3}H]- vesamicol. This ligand has affinity for a unique protein product called the "vesamicol binding protein" in noncholinergic neuron (Hicks et al., 1991). Meyer et al. (1993) reported that the highest B_{max} values for both high- and low-affinity site of [^{3}H]-vesamicol were observed from P2 to synaptic vesicle fraction and this low-affinity binding might be in soluble brain fraction. Furthermore, vesamicol itself also possesses high affinity for sigma receptors (Custers et al., 1997; Efange et al., 1995) and α-adrenergic blocking activity (Wannan et al., 1991). For this reason, ligands that are needed have a high specificity and high affinity for the vesamicol receptor.

To evaluate the distribution of cholinergic neuronal distribution and its loss in living human brain with AD, many efforts have focused on developing vesamicol derivatives as radiotracers using single SPECT and PET: Examples include benzovesamicols ((-)-5-[^{123}I]-iodobenzovesamicol, [^{123}I]-IBVM, Jung et al., 1990; (-)-5-[^{11}C]-methylaminobenzovesamicol, [^{11}C]-MABV, Mulholland and Jung, 1992; (-)-5-[^{18}F]-fluoroethoxybenzovesamicol, [^{18}F]-FEOBV, Mulholland et al., 1993), and nonsymmetrical bipiperidyls ([^{123}I]-metaiodobenzyltrozamicol, [^{123}I]-MIBT, Efange et al., 1993; [^{18}F]-parafluorobenzyltrozamicol, [^{18}F]-FBT, Efange et al., 1994). The common structure of these compounds is piperidine ring. The piperidine ring of vesamicol is important structure for high affinity to vesamicol receptor on VAChT (Rogers et al., 1989). Efange et al. (1997) reported modification of the piperidine ring, which replaced the piperidine ring with a tropane ring, and did not lead to a more potent affinity for VAChT.

In our other attempt to perform modification of piperidine ring, we selected piperazine analogs which replaced piperidine ring of (-)-vesamicol with piperazine ring. Rogers et al. (1989) reported some piperazine analogs testing for binding to vesamicol receptors of *Torpedo* cholinergic synaptic vesicle. They suggested that the replacement of the piperidine ring by piperazine ring lowers potency of the binding. On the other hand, an addition of benzene ring to cyclohexanol of vesamicol, benzovesamicol, causes an 18-fold increase of affinity of (-)-vesamicol (Rogers et al., 1993). The benzovesamicol derivative aminobenzovesamicol has higher affinity than benzovesamicol and displays high selectivity for vesamicol receptors to sigma receptors (Efange et al., 1995). In a human SPECT study, an analog with radioiodine, (-)-5-[^{123}I]-iodobenzovesamicol ([^{123}I]-IBVM), shows decreased accumulation of several brain areas in AD patients (Kuhl et al., 1996). Because of a tendency for activity of benzovesamicols to have higher activity than the vesamicol, we attempted to synthesize the piperazine analog of iodobenzovesamicol, trans-5-iodo-2-hydroxy-3-[4-phenylpiperazinyl] tetralin (DRC140).

In this study, we investigated the pharmacological characterization of the piperazine analog, DRC140, the distribution of this ligand in vivo, and studied whether this compound is a specific ligand to detect VAChT in vitro and in vivo. The goal of this investigation was to find an ideal ligand, which has a high specificity and affinity and rapidly achieves equilibrium after i.v. administration, for clinical evaluation and mapping of acetylcholine neurons as an iodine-123-labeled agent.

MATERIALS AND METHODS

Synthesis and radiolabeling of DRC140

(±)-*Trans*-5-Amino-2-hydroxy-3-(4-phenyl-1-piperazinyl) tetralin (DRC140-NH_2) was synthesized as previously reported (Jung et al., 1990). Briefly, 1-phenylpiperazine (1.55 g) was added to a solution of N-(trifluoroacetyl)-1-amino-5,8-dihydronaphthalene oxide (950 mg) (Rogers et al., 1989) in ethanol (12.5 mL). After the solution was refluxed for 20 h, the reaction mixture was kept at room temperature to produce a crystallized solid for 24 h. The solid was collected by filtration and dissolved in CH_2Cl_2. The crude product was purified by silica gel chromatography with CH_2Cl_2/ethylacetate (9:1). The solvent was removed under high vacuum to provide the white solid (DRC140-NH_2).

A solution of $NaNO_2$ (27 mg) in water (2 mL) was added to a solution of DRC140-NH_2 (120 mg) in acetic acid (2 mL) and concentrated HCl (1 mL) below 10°C. The mixture was stirred for 20 min. A solution of KI (74 mg) and I_2 (57 mg) in water (1 mL) was added the reaction mixture below 10°C. The resulting mixture was stirred for 3 h below 10°C and was kept overnight at room temperature. The reaction mixture was extracted with CH_2Cl_2. The organic layer was evaporated under reduced pressure and the crude product was purified by flash chromatography on silica gel with CH_2Cl_2/ethylacetate (95:5). The solvent was removed under high vacuum to provide the solid (racemic DRC140):^{1}H-NMR ($CDCl_3$) δ 2.90–2.62 (m,5H), 3.09–3.00 (m,2H), 3.30–3.14 (m,5H), 3.48 (q, 1H, J = 20.5 Hz), 3.19–3.84 (m,1H), 4.16(s,1H), 6.94–6.83 (m,4H), 6.97 (d, 1H, J = 8.30 Hz), 7.11 (1H, d, J = 7.81 Hz), 7.31–7.14 (m,2H), 7.71 (d, 1H, J = 7.81 Hz); MS(FAB) m/z 435 ($M+H^+$).

The mixture of diastereomeric ester of (+)- or (-)-DRC140 was produced by treating (±)-DRC140 with (-)-α-methoxy-α-trifluoromethylphenylacethyl chloride. This reaction mixture was purified by flash column chromatography on silica gel with CH_2Cl_2. The less polar compound was obtained as (+)-DRC140-ester and the polar compound as (-)-DRC140-ester. The esters were hydrolyzed 4 N NaOH to produce (-)- or (+)-DRC140.

[^{125}I]- or [^{123}I]-DRC140 were prepared by oxidative radioiododestannylation of tri-n-butyltin precursors, which were synthesized by the method of Van Dort et al. (1993). A solution of [^{125}I] NaI (7.5 mCi) or [^{123}I] NaI (40 mCi) and 0.64% peroxyacetic (40 μL) acid was added to a vial containing the tri-n-butyltin precursor of (-)-DRC140 (50 μg). After 1 min at room temperature, the reaction was stopped with of aqueous 100 mg/mL $Na_2S_2O_5$ solution (20 μL). The mixture was passed through a Sep-Pak C18 light column eluted with ethanol and the ethanol evaporated under reduced pressure. The residue was purified by HPLC (Shiseido AG 120, Tokyo, Japan; methanol/water/triethylamine = 85:15:0.2 as the mobile phase; flow rate 0.8 mL/min). [^{125}I]-DRC140 was obtained by evaporation under a nitrogen stream. Both radiochemical purities were greater than 98% and the specific activities were about 2,200 Ci/mmol for [^{125}I]-DRC140 and 12,000 Ci/mmol for [^{123}I]-DRC140.

Animals

Male Wistar rats and guinea pigs obtained from Japan SLC (Shizuoka, Japan) were housed in groups of five to six or two animals in cages with free access to food and water and maintained on a 12/h light/dark cycle. All rats weighed between 170–250 g at the time of preparation of tissue homogenates and biodistribution studies. All guinea pigs weighed between 300–500 g at the time of preparation of tissue homogenate.

Subcellular fractionation

Subcellular fractionations were performed using the published method (Huttner et al., 1983) for isolation and purification of synaptic vesicles from rat brain. In brief, adult male Wistar rats were sacrificed by decapitation and their brains quickly removed from the skull. Brains without cerebellum were homogenized in a glass-Teflon homogenizer using 12 strokes at 1,000 rpm in ice-cold buffered 0.32 M sucrose containing 4 mM HEPES-NaOH buffer, pH 7.4. The homogenate was centrifuged at 1,100*g* for 10 min. The resulting pellet (P1) was discarded and the supernatant was collected and centrifuged at 9,200*g* for 15 min. The supernatant was removed and the pellets (P2) were resuspended in buffered 0.32 M sucrose and centrifuged at 10,500*g* for 15 min. The pellet (P3) was suspended 25 mL buffered sucrose (synaptosome fraction). In order for hypo-osmotic lysis of synaptosomes to occur, the suspension was diluted with 9 vol of ice-cold water and immediately homogenized with three strokes in a Dounce homogenizer. To this suspension was added 1 M HEPES-NaOH buffer (pH7.4) to a final concentration of 7.5 mM HEPES and incubated at 4°C for 30 min. The lysate was centrifuged for 20 min at 25,500*g* and separated from pellet (P4). The supernatant was centrifuged for 2 h in a HITACHI RP45 rotor at 45,000 rpm. The supernatant was discarded. The resulting pellets (crude vesicle) were resuspended in 2 ml of 30 mM buffered sucrose containing 4 mM HEPES, and further homogenized by passing five times back and forth through a 25-gauge needle attached to a 10 ml-disposable syringe. The suspension was loaded on a discontinuous sucrose / 4 mM HEPES, pH 7.4, gradient, differing in concentration by 0.2 M and varying from 0.4 M at the top to 1.2 M at the bottom of the gradient. The sucrose layer of 0.4 M was centrifuged at 53,500*g* for 2 h (purified synaptic vesicle). Fractions containing VAChT protein were detected by the following immunoblotting method using antirat VAChT protein and collected by centrifugation at 45,000 rpm for 2 h. All steps were carried out at 4°C. The final fraction pellets were resuspended in assay buffer (50 mM Tris, 120 mM NaCl, 5 mM KCl, 2 mM $MgCl_2$, 1 mM $CaCl_2$, pH 7.4). Protein concentrations were determined with a protein assay kit (Bio-Rad, Cambridge, MA) using bovine serum albumin as a standard. VAChT protein in each subcellular fraction was detected with the following method. Ten micrograms of protein from the fractions were resolved by dodecyl sulfate-polyacrylamide gel electrophoresis (10% polyacrylamide) and then proteins transferred for 1 h to nitrocellulose membranes. The membranes were blocked by 10 mM PBS containing 5% nonfat-dry milk and 0.1% Tween 20 (PBS-Tween) for immunoblots for 1 h. After blocked membranes were incubated with antiserum against VAChT (1:3,000; Calbiochem, Cambridge ,MA) in PBS-Tween with 0.2% gelatin overnight at 4°C, they were then incubated with a secondary rabbit antigoat antibody conjugated with horseradish peroxidase (1:10,000; Chemicon International; Temecula, CA) for 45 min at room temperature. Immunoreactivity was detected by enhanced chemiluminescence system (ECL, Amersham, Cleveland, OH) as described by the manufacturer.

In vitro binding assays of [^{125}I]-DRC140

Binding assays were conducted to determine the binding properties of [^{125}I]-DRC140. Rates of association and dissociation of [^{125}I]-DRC140 were determined at 37°C using P2 fraction of rat brain in 50 mM Tris-HCl buffer, pH 7.4, containing 120 mM NaCl, 5 mM KCl, 2 mM $CaCl_2$, 1 mM $MgCl_2$. The association kinetics was determined at 37°C by adding 0.2 nM [^{125}I]-DRC140 at different times before filtration. The disso-

ciation kinetics were determined by an addition of 50 μM (-)-vesamicol at different times before filtration to the P2 fractions preincubated for 3 h at 37°C in the presence of 0.2 nM [^{125}I]-DRC140. In saturation assays, various concentrations (0.03–1.3 nM) of [^{125}I]-DRC140 were incubated in duplicate with each fraction at 37°C for 3 h. Final concentrations of components in the assay solution were 50 mM Tris-HCl buffer. Nonspecific binding was defined by incubation in the presence 20 μM (-)-vesamicol. The competition assays were performed as follows. The fractions were incubated with 0.2 nM [^{125}I]-DRC140 and various concentrations of competing compounds at 37°C for 3 h in 50 mM Tris–HCl buffer. Nonspecific binding was defined using 20 μM (-)-vesamicol.

Incubation was terminated by rapid filtration through Whatman GF/B filters previously soaked in 2% polyethylenimine using a Brandel Cell Harvester. The filters were washed three times with 2 ml of ice-cold Tris-HCl buffer and counted using a Minaxi gamma counter (Packard).

Sigma receptor binding assays

Sample preparation for ligand binding assays

Guinea pigs and rats were sacrificed by decapitation. The guinea pig brain or rat liver was quickly removed. Crude P2 membrane fraction was prepared from the brain without cerebellum of guinea pig or the liver of rat using a published method (Matsumoto et al., 1995). The tissues were homogenized in a glass-Teflon homogenizer using 10 strokes at 1,000 rpm in ice-cold buffered 0.32 M sucrose in 10 mM Tris-HCl, pH 7.4 (Tris-sucrose buffer) in a volume of 10 mL/g wet tissue weight. The homogenates were centrifuged at 4°C at 1,000*g* for 10 min and supernatants saved. The pellets were resuspended in 2 mL/g Tris-sucrose buffer and centrifuged at 4°C at 1,000*g* for 10 min. The supernatants from both 1,000*g* spins were combined and centrifuged at 4°C at 31,000*g* for 15 min. The pellets were resuspended in 10 mM Tris-HCl, pH 7.4, in a volume of 3 ml/g of tissue and the suspensions were incubated for 15 min at 25°C. Following centrifugation at 31,000*g* for 15 min, the pellets were resuspended in 10 mM Tris-HCl, pH 7.4, to a final concentration of 1.53 ml/g tissue. The aliquots stored at −80°C until use.

Binding to sigma receptors

The affinity of DRC140 for sigma-1 receptors was determined using a sigma-1-selective ligand [^{3}H]-(+)-pentazocine and brain P2 membranes of guinea pig. Briefly, the membranes (300 μg protein) were incubated with 3 nM [^{3}H]-(+)-pentazocine and various concentrations (0.05–10,000 nM) of DRC140. Incubation was carried out in a total volume of 0.3 ml of 50 mM Tris-HCl, pH 8.0 for 120 min at 25°C. Nonspecific binding was determined in the presence of 10 μM haloperidol.

Sigma-2 binding assay was determined using rat liver P2 membranes (200 μg protein) and [^{3}H]-1,3-di-o-tolyguanidine ([^{3}H]DTG). These were incubated with 3 nM [^{3}H]-DTG in the presence of 200 nM (+)-SKF10,047 to mask sigma-1 sites. Nonspecific binding was evaluated in the presence of 10 μM haloperidol.

Assays were terminated by dilution with 2 ml ice-cold 10 mM Tris-HCl, pH 8.0, and vacuum filtration through Whatman GF/B filter glass fiber filters previously soaked in 0.5% polyethyleneimine using the Inotech cell harvester system (Inotech, Switzerland). The filters were then washed twice with 1 ml of ice-cold buffer. For measurement with MicroBeta (EG&G Wallac, Finland), the filters were dried and meltable solid scintillator, MeltiLex B/HS, was melted into the filters.

Data analysis

Equilibrium dissociation constants (K_d) and receptor densities (B_{max}), inhibitory concentration at 50% (IC_{50}) values, and kinetic parameters (association constant k_{on} and dissociation constant k_{off}) were determined by the nonlinear curve-fitting method using EXCEL (Microsoft) incorporated Solver program. The dissociation constants of inhibitors (K_i) were calculated with the equation of Cheng and Prusoff (1973).

In vivo binding studies

Rats received an i.v. injection of 1.5 MBq [^{123}I]-DRC140 via the tail vein. After various specified time intervals, the animals were sacrificed by decapitation under anesthesia and a blood sample was collected into a heparinized test tube. The brain was removed and immediately dissected on ice: frontal cortex, occipital cortex, hippocampus, striatum, cerebellum, and other regions were weighed. The peripheral tissue samples were excised from each animal and weighed. The radioactivity in each tissue was measured using Minaxi gamma counter (Packard). The %dose/gram of tissue was determined by a comparison of the tissue counts to suitable diluted aliquots of the injected [^{123}I]-DRC140.

In order to study specific binding of [^{125}I]-DRC140 in vivo using autoradiographic analysis, a rat was i.v. injected with [^{125}I]-DRC140 and sacrificed by decapitation at 90 min post-i.v. injection of the radiotracer. The brain was removed and immediately frozen. Horizontal and coronal sections were cut by a cryostat. The sections were thaw-mounted onto slides, air-dried, and placed on an imaging plate in X-ray cassettes (Fuji Film, Tokyo, Japan). After exposure the plates were scanned using a Fuji Bioimaging Analysis System (BAS-1800; Fuji). The measurements were taken from four or five consecutive slices per rat for the brain regions of interest based on the atlas of Paxinos and Watson (1986). The densities of the uptake were transformed according to the optical density of the calibrated standards. The relative values were expressed

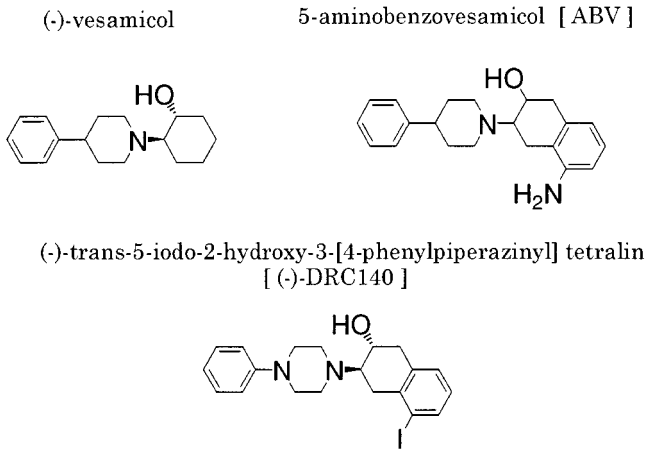

Fig. 1. Chemical structures of vesamicol derivatives.

in ratio of the region to cerebellum. A blocking study was performed by i.v. injection of 0.5 mg/kg of (-)-vesamicol 3 min prior to the administration [^{125}I]-DRC140.

Drugs

The following drugs were obtained from Research Biochemicals International (Natick, MA) and used in the competition study: (-)- or (+)-vesamicol, 1,3-di(2-tolyl-)guanidine (DTG), haloperidol, ketanserin, (-)-3-quinuclidinyl benzilate (QNB), eserine, 5-methylurapidil, 1-(2-methoxyphenyl)-4-[4-(2-phthalimido)butyl]piperazine (NAN-190), 1-methyl-N-(8-methyl-8-azabicyclo[3.2.1]-oct-3-yl)-1H-indazole-carboxamide (LY-278,584), (-)-propranolol, R,S-[3-[1-[[(3,4-dichlorophenyl)acetyl]methylamino]2-2(1-pyrrolidinyl)ethyl]phenoxy]-acetic acid (ICI204,448), 1-(4-aminophenyl)-4-methyl-7,8-methylenedioxy-5H-2,3-benzodiazepine (GYKI52466), 5,7-dichlorokynurenic acid, and reserpine. 5-Aminobenzovesamicol (ABV) was synthesized as previously reported (Roger et al., 1989).

RESULTS

Binding assays in subcellular fractions

Purification of synaptic vesicles preparation was carried out from rat whole brain without cerebellum as previously described (Huttner et al., 1983). Crude vesicles were centrifuged in discontinuous sucrose gradient to produce purified vesicles as described by Whittaker et al. (1964). The VAChT in each fraction was confirmed by Western blot analysis. As shown in Figure 2, the specific antibody against VAChT protein recognized a major band of ~70 kDa in all fractions from rat brain. A slight increase in VAChT was observed from homogenate through P2, P3, and P4 fractions. The VAChT was markedly enriched in crude vesicle fractions and further purified in 0.4 M fraction in sucrose gradient. A kinetic binding characteristic of [^{125}I]-DRC140 was investigated in rat P2 fraction. The

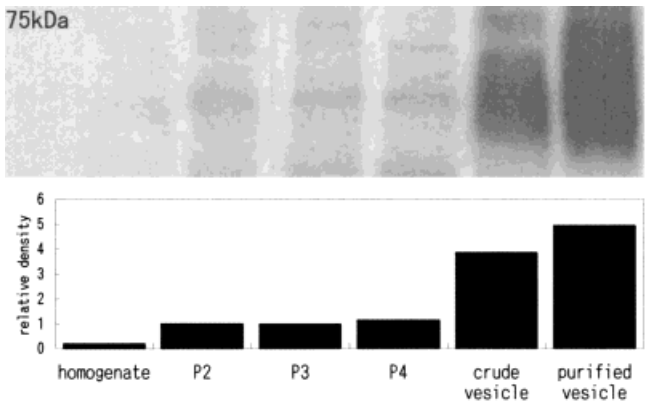

Fig. 2. Immunoblots (top) and quantitative relative density (bottom). The VAChT in each subcellular fraction was detected by antiserum against VAChT. The blot shows ~70 kDa in all fractions. The relative densities expressed the ratio of density of each fraction to that of P2 fraction.

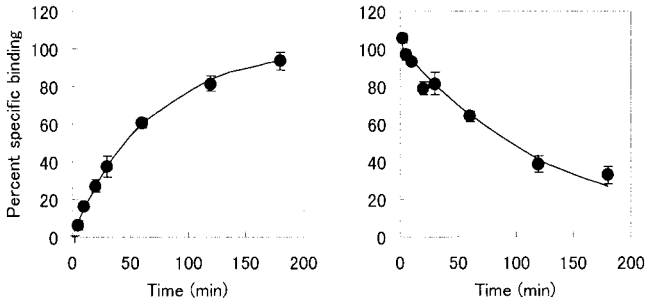

Fig. 3. Association and dissociation [^{125}I]-DRC140 binding to P2 fraction of rat brain. The binding property of [^{125}I]-DRC140 was measured at 37°C after different incubation times. Dissociation was measured by adding 50 μM (−)vesamicol to P2 fraction at different time before filtration. Each point represents mean ± SD of four experiments with duplicate determinations.

association and dissociation time courses are shown in Figure 3. After 180 min at 37°C, >90% of maximal specific [^{125}I]-DRC140 binding was reached (k_{on} = 0.040 $min^{-1} \cdot nM^{-1}$). The dissociation rate constant k_{off} of [^{125}I]-DRC140 binding was 0.0075 min^{-1} in the P2 fraction.

A saturation experiment was performed in P2, crude synaptic vesicle, and purified synaptic vesicle fractions. Because [^{125}I]-DRC140 binding reached plateau levels at 180 min at 37°C, the assay was carried out incubation for 180 min at 37°C. [^{125}I]-DRC140 binding was observed in all fractions and saturation with increasing amounts of the radioligand (0.03–1.3 nM) (Fig. 4, inset). The K_d and B_{max} values were obtained by Scatchard plot (Fig. 4) and these values are shown in Table I. A single site binding was observed for P2 fraction with K_d = 0.41 ± 0.111 nM and B_{max} = 187 ± 53.3 fmol/mg protein. K_d = 0.34 ± 0.031 nM and B_{max} = 821 ± 78.6 fmol/mg protein were obtained in crude vesicle fraction. The B_{max} in synaptic vesicle fraction (1,751 ± 92.6 fmol/mg protein) was nine times higher than that in P2 fraction. However, the K_d values

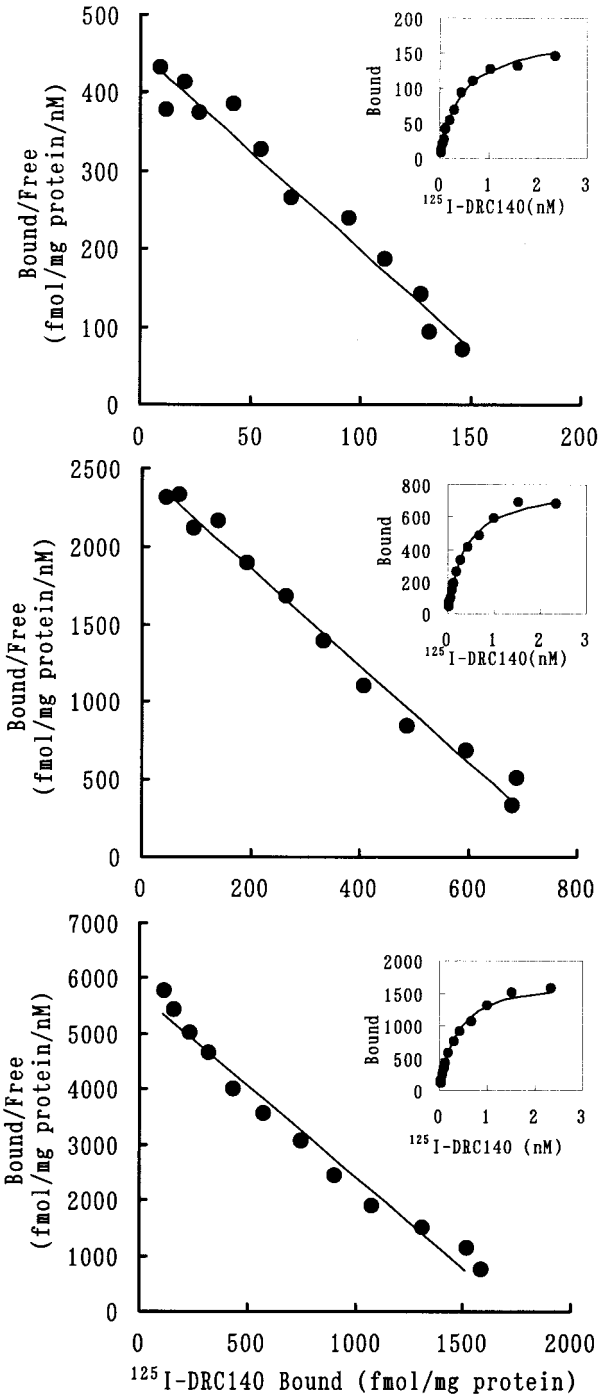

Fig. 4. Scatchard analysis of [^{125}I]-DRC140 binding to P2 fraction (top panel), Crude vesicle (middle panel) and purified synaptic vesicle fraction (bottom). The insets show the saturation binding of [^{125}I]-DRC140. Nonspecific binding was defined with 20 μM (−)-vesamicol.

(0.31 ± 0.009 nM) in purified synaptic vesicles was not different from the other fractions (Table I).

Competition experiments of specific [^{125}I]-DRC140 binding with P2 or the purified synaptic vesicle fraction were studied using various inhibitors (Table II, Fig. 5). Unlabeled (-)-DRC140 and 5-aminobenzovesamicol

TABLE I. Affinities of [^{125}I]-DRC140 binding in subcellular fractions of rat brain

	B_{max} (fmol/mg protein)	K_d (nM)
P2	187 ± 58.3	0.41 ± 0.111
Crude vesicle	821 ± 78.6	0.34 ± 0.031
Synaptic vesicle	1751 ± 92.6	0.31 ± 0.009

Subcellular fractions were prepared from whole rat brain without cerebellum as described in Methods. Each fraction was incubated for 3 h at 37°C with different concentrations of [^{125}I]-DRC140 (0.03–2.3 nM). Nonspecific binding was defined with 20 μM (−)-vesamicol. The data are the mean ± SD of three experiments with duplicate determinations.

(ABV) displaced the specific binding of [^{125}I]-DRC140 to the P2 fraction with K_i values of 1.21 ± 0.075 nM and 0.91 ± 0.141 nM, respectively. The K_i of these compounds for the purified synaptic vesicle fraction was similar to that of the P2 fraction. We found that DRC140 displayed high stereoselectivity. The K_i value of (-)-DRC140 was 46 times more potent than the (+)-isomer. Moreover, (-)-vesamicol was >120 times more potent than (+)-vesamicol. Hill coefficients of (-)-vesamicol and haloperidol were shown to be 0.66 ± 0.037 and 0.64 ± 0.103, respectively. These inhibitors also showed that the nHs were approximately one for purified synaptic vesicle. Compounds that bind to sigma/dopamine D_2 or serotonin 5-HT_2 receptor, such as haloperidol, DTG, and ketanserin, had a 700–2,700-fold lower potency of inhibitory binding to P2 than (-)-DRC140, as well as binding to synaptic vesicle fraction. Other compounds that inhibit the specific receptors, enzyme, and transporter, such as 5-HT_{1A}, 5-HT_3, muscarin, α-,β-adrenergic, κ-opioide, α-amino-3-hydroxy-5-methylisoxazole-4-propionate (AMPA) or kinate, glycine, acetylcholine esterase, and mono amine uptake inhibitor did not inhibit the binding of [^{125}I]-DRC140 in P2 fraction (K_i > 50,000 nM).

The different vesamicol compounds (Fig. 1) were tested in vitro binding studies to assess their affinities at sigma-1, sigma-2 receptors (Table III). There were small differences among the affinities of each enantiomer of DRC140 at the sigma-1 and sigma-2 receptors and vesamicol at sigma-2 receptors. Both (-)- and (+)-DRC140 had much lower affinity of DRC140 for sigma-1 and sigma-2 receptors than affinities of vesamicol and racemic ABV.

Biodistribution in rat

The time–activity data of [^{123}I]-DRC140 in rat brain regions, blood (%dose/g tissue), and peripheral organs (%dose) are shown in Table IV. The radioligand readily crossed the blood–brain barrier and high accumulation of radioactivity was detected in all brain regions at 2 min after the injection. There was a high accumulation of radioactivity in the striatum (1.895 %dose/g tissue), with maximum accumulation reached at 5 min postinjection. The accumulation of radiotracer in this area showed a slower clearance of radioactivity than the other areas. Time–activity curves of frontal cortex, occipital cortex, and hippocampus were similar. The ac-

TABLE II. Potencies of various compounds to inhibit the binding of [^{125}I]-DRC140 to subcellular fractions of rat

P2 fraction inhibitor	Receptor or enzyme	Ki(nM) mean ± SD	Hill coefficient mean ± SD
(−)-DRC140	vesamicol	1.21 ± 0.075	0.98 ± 0.026
(+)-DRC140		55.9 ± 8.56	0.84 ± 0.054
(±)-ABV	vesamicol	0.91 ± 0.141	0.98 ± 0.130
(−)-vesamicol	vesamicol	40.7 ± 9.89	0.66 ± 0.037
(+)-vesamicol		>5,000	
DTG	σ	3052 ± 606	0.77 ± 0.075
haloperidol	σ/D_2	849 ± 18	0.64 ± 0.103
NAN-190	5-HT_{1A}	>5,000	
ketanserin	5-HT_2	862 ± 119	0.80 ± 0.086
LY-278,584	5-HT_3	>5,000	
QNB	muscarinic	>5,000	
eserine	acetylcholine esterase	>5,000	
5-methylurapidil	α_1-adrenergic	>5,000	
(−)-propranolol	β-adrenergic	>5,000	
ICI204,448	κ-opioide	>5,000	
GYKI52466	AMPA/kinate	>5,000	
5,7-dichlorokynurenic acid	glycine	>5,000	
reserpine	mono amine uptake site	>5,000	

Purified vesicle inhibitor	Ki(nM) mean ± SD	Hill coefficient mean ± SD
(−)-DRC140	1.11 ± 0.306	1.06 ± 0.068
(±)-ABV	1.32 ± 0.060	1.07 ± 0.031
(−)-vesamicol	36.1 ± 2.34	0.93 ± 0.023
DTG	3312 ± 163	0.91 ± 0.037
haloperidol	778 ± 30	0.96 ± 0.009
ketanserin	954 ± 28	0.86 ± 0.023

The data are the mean ± SD of three experiments with duplicate determinations.

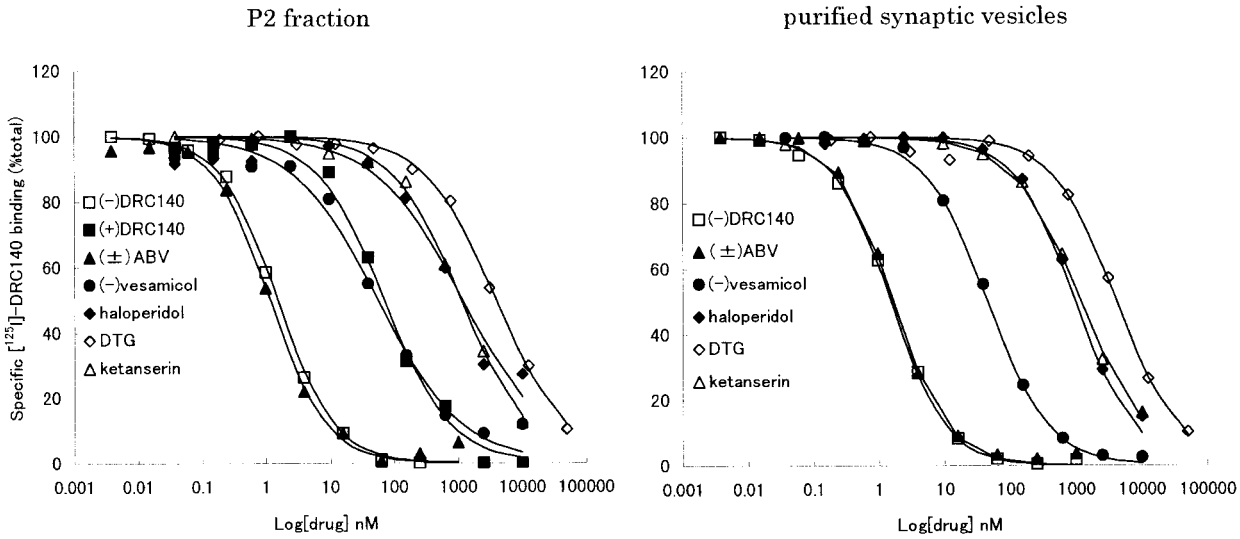

Fig. 5. Displacement curves of specific binding of [^{125}I]-DRC140 to the subcellular fraction of rats. Each of the fractions was incubated with 0.2 nM [^{125}I]-DRC140 and increasing amounts of various inhibitors.

cumulation in cerebellum decreased at a more rapid rate than other areas. The distribution of radioactivity in each region of rat brain at 240 min after injection showed the following order: striatum (0.343 %dose/g tissue), frontal cortex (0.108 %dose/g tissue), hippocampus (0.099 %dose/g tissue), occipital cortex (0.090 %dose/g tissue), and cerebellum (0.041 %dose/g tissue). The ratios of striatum-to-cerebellum and frontal cortex-to-cerebellum were 1.1 and 1.2, respectively, in rat brain at 2 min. These ratios gradually increased in a chronological order after injection and attained 2.6 for the cortex and 8.2 for the striatum at 4 h.

High uptake of radioactivity was observed in the small intestine, with a maximum accumulation 59% dose at 90 min. The radioactivity of large intestine rose dramatically at 240 min, in agreement with the decrease of activity in small intestine at that time point. The main route of excretion of [^{123}I]-DRC140 likely

TABLE III. Potencies of vesamicol derivatives to inhibit the binding of [^{3}H]-(+)-pentazocine in guinea pig brain (σ1) and [^{3}H]-DTG binding in rat liver (σ2)

	σ_1 receptor IC_{50} ± SD (nM)	σ_2 receptor IC_{50} ± SD (nM)
(−)-vesamicol	66.5 ± 5.03	45.6 ± 2.34
(+)-vesamicol	19.0 ± 1.64	40.3 ± 1.07
(−)-DRC140	3,371 ± 210	2,120 ± 145
(+)-DRC140	3,336 ± 340	1,940 ± 92.5
(±)-ABV	157 ± 11.4	174 ± 15.9

The data are the mean ± SD of three experiments with duplicate determinations.

seems to be a hepatobiliary system. In order to evaluate the in vivo deiodination of [^{123}I]-DRC140, we removed the thyroid gland of each animal and measured its radioactivity. This radioactivity remained at a constant at low level for each sampling time.

Figure 6 shows ex vivo autoradiographic localization of [^{125}I]-DRC140 binding sites in rat brain at 90 min after injection. High accumulation was observed in the striatum, interpeduncular nucleus, olfactory tubercle, basolateral amygdaloid, and facial nerve. Moderate levels of binding were found in cortex and hippocampus, whereas little accumulation was shown in cerebellum (Figs. 6A,C, 7A). The distribution of binding sites correlated with that of the regional VAChT protein (Schäfer et al., 1998; Ichikawa et al., 1997; Arvidsson et al., 1997). Pretreatment with VAChT inhibitor (vesamicol 0.5 mg/kg) at 3 min before injection of the radioligand markedly reduced the uptake of [^{125}I]-DRC140 in all high accumulation regions (Figs. 6B, 7B). Moreover, the region-to-cerebellum ratios in rats pretreated with (-)-vesamicol were close to unity. In order to confirm whether pretreated (-)-vesamicol might affect the distribution in cerebellum, the densities were normalized in %dose/g tissue by I-125 standards. There was no significant difference of radioactivity in cerebellum between control (0.100 ± 0.0212 %dose/g tissue) and pretreated rats (0.104 ± 0.0151 %dose/g tissue).

DISCUSSION

We investigated whether a piperazine analog, (-)-DRC140, was specific ligand to detect the VAChT in vitro and in vivo. In order to clarify the binding of [^{125}I]-DRC140 to the vesamicol receptor, we conducted in vitro binding studies using purified synaptic vesicles from rat brain. In saturation binding studies, [^{125}I]-DRC140 we observed a high binding affinity in all subcellular fractions of rat brain. The highest B_{max} for [^{125}I]-DRC140 was observed in the purified synaptic vesicle fraction (1,751 fmol/mg protein), followed by the crude vesicle (821 fmol/mg protein), and then the P2 fraction (185 fmol/mg protein). There was almost a 9-fold difference between the B_{max} of binding to P2 fraction and to the purified synaptic vesicle. According to the results of the Western blot analysis, the densitmetric scans of immunoreactivity of anti-VAChT antibody to each fraction indicated that the concentration of VAChT protein was clearly increased by our method of purification of synaptic vesicles (Fig. 2). The increment in binding of [^{125}I]-DRC140 in the more purified fraction was in accordance with the increase in the immunoreactive signal against VAChT. Our results are consistent with the binding of [^{125}I]-DRC140 to the VAChT on synaptic vesicles.

The affinity constant (K_d) for vesamicol receptors in the P2 fraction was similar to the affinity of highly purified synaptic vesicular fraction (K_d = 0.3 nM), with the best fit described by a one-site model. These observations support that [^{125}I]-DRC140 has a high-affinity site in synaptic vesicle and the K_d for vesamicol receptors may not be influenced by other cytoplasm components.

In the competition studies, cold (-)-DRC140 and (±)-ABV strongly displaced [^{125}I]-DRC140 binding to P2 fraction and purified vesicles. These K_i values for the P2 fraction were almost the same inhibition constants for both compounds in the vesicle fractions. A comparison of the inhibition constants of each enantiomer of DRC140 and vesamicol resulted that (-)-DRC140 was

TABLE IV. Biodistribution of [^{123}I]-DRC140 in rat after i.v. injection of the tracer

	2 min	5 min	10 min	20 min	40 min	90 min	240 min
%dose/g							
Cerebellum	1.338 ± 0.179	1.544 ± 0.346	1.137 ± 0.170	0.684 ± 0.028	0.353 ± 0.043	0.131 ± 0.003	0.041 ± 0.006
Hippocampus	1.122 ± 0.127	1.355 ± 0.200	1.193 ± 0.179	0.825 ± 0.055	0.560 ± 0.074	0.267 ± 0.022	0.099 ± 0.023
Striatum	1.463 ± 0.117	1.895 ± 0.305	1.775 ± 0.326	1.537 ± 0.080	1.423 ± 0.233	0.813 ± 0.143	0.343 ± 0.060
Frontal cortex	1.552 ± 0.213	1.683 ± 0.254	1.359 ± 0.194	0.911 ± 0.053	0.619 ± 0.104	0.306 ± 0.026	0.108 ± 0.012
Occipital cortex	1.594 ± 0.097	1.681 ± 0.171	1.381 ± 0.245	0.872 ± 0.030	0.577 ± 0.077	0.280 ± 0.037	0.090 ± 0.011
Other cerebral region	1.314 ± 0.146	1.618 ± 0.298	1.330 ± 0.196	0.923 ± 0.036	0.626 ± 0.077	0.310 ± 0.023	0.109 ± 0.019
Blood	0.897 ± 0.055	0.720 ± 0.128	0.500 ± 0.095	0.357 ± 0.010	0.212 ± 0.018	0.134 ± 0.005	0.116 ± 0.013
%dose							
Whole brain	2.388 ± 0.223	2.814 ± 0.478	2.216 ± 0.327	1.486 ± 0.067	1.019 ± 0.142	0.505 ± 0.046	0.168 ± 0.023
Heart	0.769 ± 0.046	0.475 ± 0.080	0.304 ± 0.027	0.194 ± 0.028	0.087 ± 0.016	0.036 ± 0.003	0.060 ± 0.010
Lungs	1.775 ± 0.137	1.330 ± 0.167	0.873 ± 0.110	0.552 ± 0.073	0.318 ± 0.031	0.150 ± 0.015	0.156 ± 0.015
Liver	8.981 ± 1.381	12.163 ± 1.952	13.832 ± 0.906	11.018 ± 0.803	6.988 ± 0.228	5.215 ± 0.488	3.241 ± 0.488
Kidneys	1.666 ± 0.318	1.318 ± 0.159	0.878 ± 0.069	0.573 ± 0.033	0.373 ± 0.011	0.238 ± 0.053	0.245 ± 0.026
Stomach	1.063 ± 0.220	1.276 ± 0.128	1.680 ± 0.266	2.288 ± 0.188	1.804 ± 0.295	0.941 ± 0.231	1.031 ± 0.221
Small intestine	3.957 ± 1.011	5.342 ± 0.748	9.547 ± 0.900	19.537 ± 0.866	36.664 ± 4.248	58.735 ± 5.420	22.657 ± 4.627
Large intestine	1.106 ± 0.306	0.941 ± 0.072	0.838 ± 0.110	0.683 ± 0.145	0.574 ± 0.072	1.210 ± 1.204	47.017 ± 3.105
Thyroid	0.072 ± 0.003	0.063 ± 0.008	0.059 ± 0.007	0.044 ± 0.013	0.036 ± 0.013	0.064 ± 0.008	0.053 ± 0.005

Radioactivities are expressed as the %dose or %dose/g of tissue. The values are the mean ± SD of determinations of four rats at each time point.

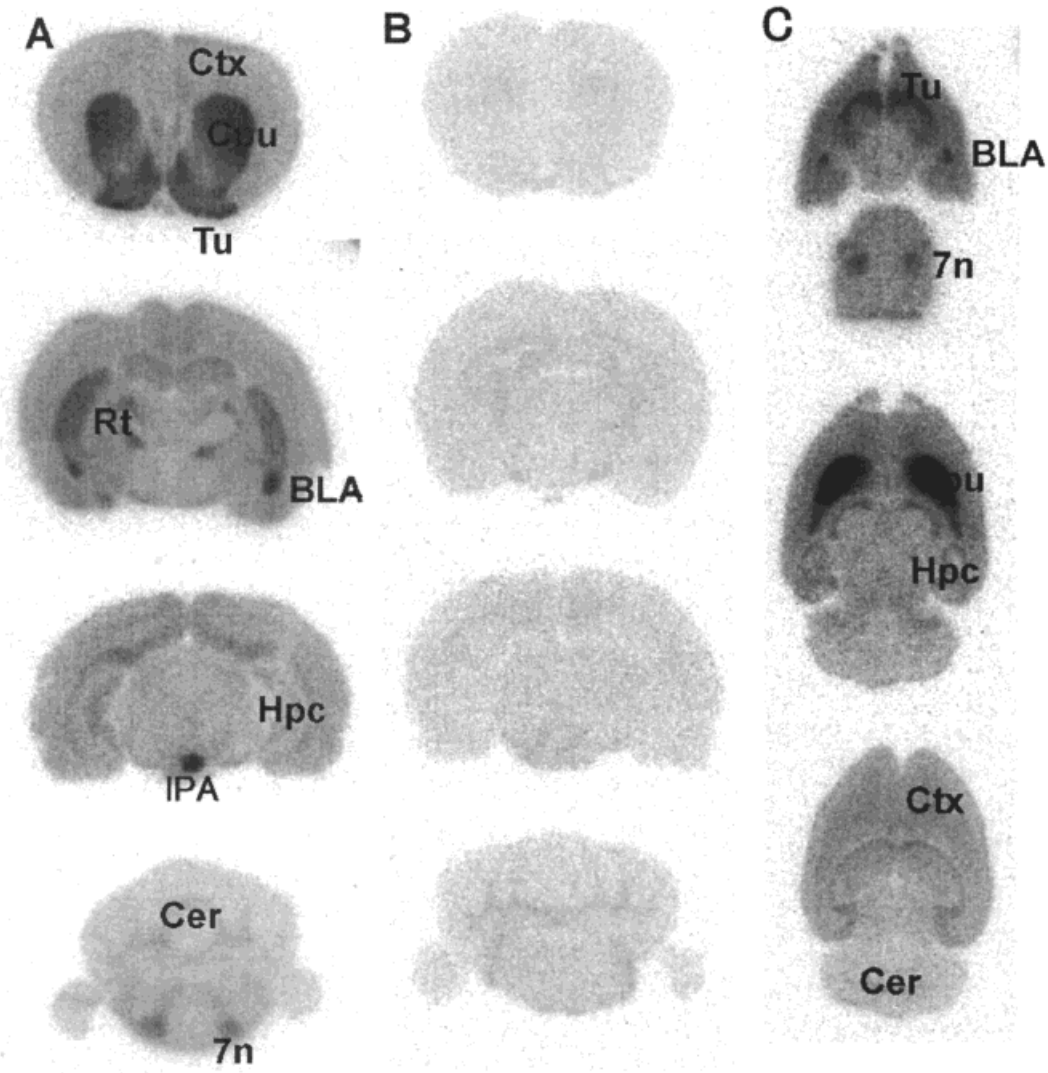

Fig. 6. Autoradiographic distribution of [^{125}I]-DRC140 rat brain at 90 min after injection in coronal (**A**) and in horizontal section (**C**). Effect of (−)-vesamicol of preinjection on the distribution of the radioactivity (**B**). (−)-Vesamicol (0.5 mg/kg, i.v.) was injected at 3 min before radiotracer administration. Tu, olfactory tubercle; Bla, basolateral amygdaloid; 7n, facial nerve; Cpu, striatum; Rt, reticular thalamus; Hpc, hippocampus; Ctx, cerebral cortex, Cer, cerebellum.

46 times more potent than (+)-isomer of DRC140. Similarly, (-)-vesamicol was >120 times more potent than that of (+)-vesamicol (Table II). Conclusively, DRC140 seemed to have the high stereoselectivity described with other vesamicol derivatives (Rogers et al., 1989).

The Hill coefficients of (±)-ABV and (-)-DRC140 were similar in the P2 fraction experiment. Each value was consistent with the value in the purified synaptic vesicle fraction. It was shown that both compounds specifically antagonized [^{125}I]-DRC140 binding in P2 fraction. Although the Hill coefficient of (-)-vesamicol was 0.93 in purified synaptic vesicles, the value was 0.66 in P2 fraction. The reasons for the difference between the value for P2 fraction and for purified vesicles might be that (-)-vesamicol was not likely to bind to the vesamicol receptor but to other interactive sites contained in the P2 fraction.

Vesamicol and its relatives have been reported to possess affinity for sigma receptors (Custers et al., 1997; Efange et al., 1995; Jung et al., 1996). For that reason, we used an inhibition assay using haloperidol and DTG as sigma receptor ligands and found lower affinity constants for the sigma ligands (K_i = 849 nM for haloperidol and K_i = 3052 nM for DTG) when compared to that of [^{125}I]-DRC140 in P2 fraction (Table II). In the purified synaptic vesicle examination, both sigma receptor inhibitors, haloperidol and DTG, showed similar antagonism to P2 fraction. Several reports described the phenomenon of low concentration of sigma receptors in synaptosome fraction in rat brain (McCann et al., 1989; McCann and Su, 1990). The inhibition of specific binding of [^{125}I]-DRC140 by the sigma ligands may not result from the competitive mechanism on sigma receptors, but may be competitive

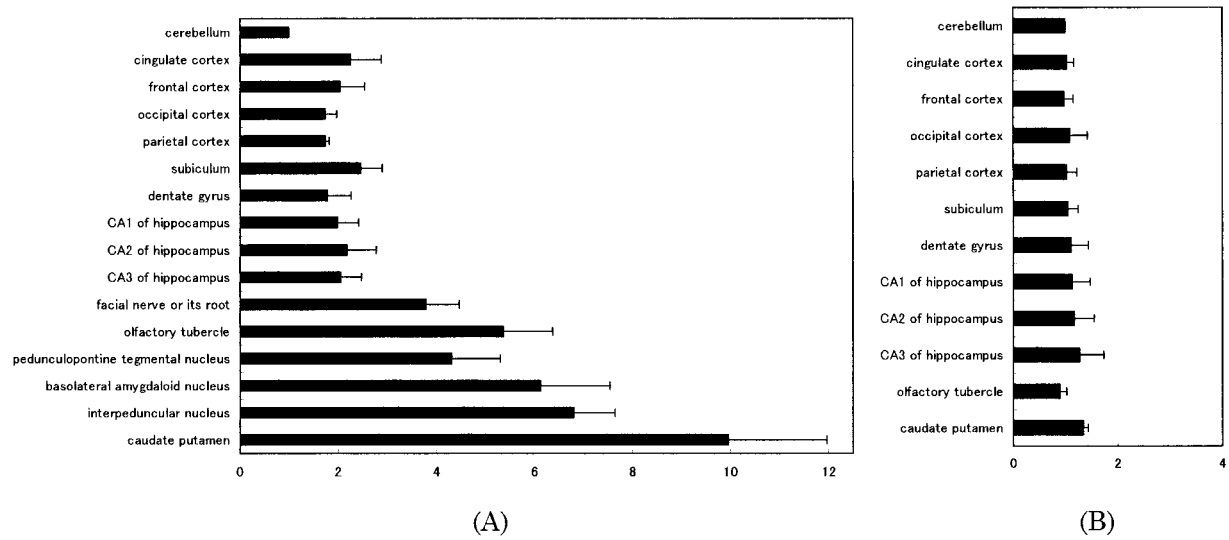

Fig. 7. Quantitative analysis of distribution of [^{125}I]-DRC140 in rat brain of control (**A**) and preinjected vesamicol (**B**). (−)-Vesamicol (0.5 mg/kg, i.v.) was injected at 3 min before radiotracer administration. The accumulations of the radioactivity were measured by autoradiography in different areas and imaging analysis. The density of the uptake was expressed in ratios to the radioactivity in cerebellum. Data are presented as mean values ± SD of density from four or five consecutive slices per rat (n = 3).

mode on vesamicol receptors. In addition, competition studies with [^{3}H]-(+)-pentazocine and [^{3}H]-DTG revealed much lower affinity of DRC140 than affinities of piperidine derivatives (i.e., vesamicol and (±)-ABV) for sigma-1 and sigma-2 receptor (Table III). Consequently, the possibility that [^{125}I]-DRC140 recognizes sigma receptors was neglected by our data.

The affinities of [^{125}I]-DRC140 for several types of neurotransmitter receptors and enzymes were also assessed using a competition method. Although K_i values for ketanserin were 862 nM in P2 fraction and synaptic vesicle fraction, the other ligands were not able to inhibit more than 50% of [^{125}I]-DRC140 specific binding at high concentrations of inhibitors (Table II).

In vivo distribution studies of [^{123}I]-DRC140 in rats showed a rapid penetration into brain, with a peak uptake at 5 min in all brain regions after injection (Table III). This labeled ligand readily crossed the blood–brain barrier and may have a suitable lipophilicity to be extracted into brain. These distribution patterns in the brain regions were similar at 5 min after injection except for the striatum. The relative accumulation in striatum was somewhat higher than that of cerebellum in the earlier period. In later periods after i.v. injection, striatum displayed the highest regional radioactivity throughout the brain regions, frontal cortex, occipital cortex, hippocampus, and cerebellum. The distribution pattern in regional brain of this tracer, DRC140, in rat was quite similar to that of radioligand of VAChT for SPECT or PET previously described in the literature (Jung et al., 1990, 1996; Efange et al., 1993, 1999).

For the ex vivo autoradiographic evaluation, the distribution and the specificity of [^{125}I]-DRC140 was assessed in vivo at 90 min after the tracer injection with and without the (-)-vesamicol pretreatment (0.5 mg/kg i.v.) (Figs. 6, 7). The autoradiogram of [^{125}I]-DRC140 showed that the highest density region was striatum, followed by interpeduncular nucleus, basolateral amygdaloid, olfactory tubercle, peduncular tegmental nucleus, and facial nerve nucleus. These data were in line with the areas which were high-density regions of VAChT (Schäfer et al., 1998; Ichikawa et al., 1997; Arvidsson et al., 1997).

For the purpose of the antagonism examination, we studied [^{125}I]-DRC140 using vesamicol-treated rats (Figs. 6, 7). A preinjection of (-)-vesamicol strikingly prevented the accumulation of [^{125}I]-DRC140, especially in the high-density regions and the resultant density was reduced to background levels, like that of the cerebellum, whose density was unaffected by either pretreatment of mock control (0.100 ± 0.0212 %dose/g tissue) or (-)-vesamicol (0.104 ± 0.0151 %dose/g tissue).

This observation is also supported by the low expression level of the VAChT, transcriptionally and translationally (Roghani et al., 1994; Bejanin et al., 1994; Ericson et al., 1994; Gilmor et al., 1998) in cerebellum. As a nonspecific reference region, the radioactivity of [^{125}I]-DRC140 in cerebellum also seems to be the case for tracer kinetic analysis in vivo.

Our data represents the first report of a piperazine derivative of vesamicol for in vitro and in vivo studies of the VAChT. As a result of binding in P2 and purified synaptic vesicle fraction, [^{125}I]-DRC140, piperazine analog of IBVM, displayed a high affinity for vesamicol receptors on the VAChT. The binding may not be influenced by other cytoplasm components. The most important conclusion from the present study is that the piperazine derivative DRC140 has a high specificity for vesamicol receptors. The inhibition studies demon-

strated that [^{125}I]-DRC140 binding was not affected by ligands for other types of receptors, enzymes, and transporters. A particular advantage of this structure, piperazine derivative, is its high selectivity for vesamicol receptors over sigma receptor. The biodistribution of DRC140 in rat shows a high brain permeability. The regional brain distribution of the ligand was consistent with the distribution of acetylcholine neuron. These findings suggest that [^{125}I]-DRC140 may be a useful tracer for in vivo SPECT studies for quantitative studies in vitro of the VAChT and may be a viable lead compound for ideal SPECT agent development.

REFERENCES

Alfonso A, Grundahl K, Duerr JS, Han H-P, Rand JB. 1993. The Caenorhabditis elegans unc-17 gene: a putative vesicular acetylcholine transporter. Science 261:617–619.

Arvidsson U, Riedl M, Elde R, Meister B. 1997. Vesicular acetylcholine transporter (VAChT) protein: a novel and unique marker for cholinergic neurons in the central and peripheral nervous systems. J Comp Neurol 378:454–467.

Bejanin S, Cervini R, Mallet J, Berrard S. 1994. A unique gene organization for two cholinergic markers, choline acetyltransferase and a putative vesicular transporter of acetylcholine. J Biol Chem 269:21944–21947.

Cheng TC, Prusoff WH. 1973. Relationship between the inhibition constant (K_i) and the concentration of inhibitor which causes 50 per cent inhibition (I_{50}) of an enzymatic reaction. Biochem Pharmacol 22:3099–3108.

Custers FGJ, Leysen JE, Stoof JC, Herscheid JDM. 1997. Vesamicol and some of its derivatives: questionable ligands for selectively labelling acetylcholine transporters in rat brain. Eur J Pharmacol 338:177–183.

Davies P, Malony AJF. 1976. Selective loss of central cholinergic neurons in Alzheimer's disease. Lancet 25:1403.

Efange SMN, Michelson RH, Khare AB, Thomas JR. 1993. Synthesis and tissue distribution of (m-[^{125}I]iodobenzyl)trozamicol ([^{125}I]MIBT): potential radioligand for mapping central cholinergic innervation. J Med Chem 36:1754–1760.

Efange SMN, Mach RH, Khare AB, Michelson RH, Nowak PA, Evora PH. 1994. p-[^{18}F]Fluorobenzyltrozamicol ([^{18}F]FBT): molecular decomposition-reconstitution approach to vesamicol receptor radioligands for positron emission tomography. Appl Radiat Isot 45:465–472.

Efange SMN, Mach RH, Smith CR, Khare AB, Foulon C, Akella SK, Childers SR, Parsons SM. 1995. Vesamicol analogues as sigma ligands: molecular determinants of selectivity at the vesamicol receptor. Biochem Pharmacol 47:791–797.

Efange SMN, Kamath AP, Khare AB, Kung M-P, Mach RH, Parsons SM. 1997. N-Hydroxyalkyl derivatives of 3β-phenyltropane and 1-methylspiro[1H-indoline-3,4'-piperidine]: vesamicol analogues with affinity for monoamine transporters. J Med Chem 40:3905–3914.

Efange SMN, Nader MA, Ehrenkaufer RLE, Khare AB, Smith CR, Morton TE, Mach RH. 1999. (+)-p-([^{18}F]Fluorobenzyl)spirotrozamicol {(+)-[^{18}F]spiro-FBT}: synthesis and biological evaluation of a high-affinity ligand for the vesicular acetylcholine transporter (VAChT). Nucl Med Biol 26:189–192.

Erickson JD, Varoqui H, Schäfer MK-H., Modi W, Diebler M-F, Weihe E, Rand J, Eiden LE, Bonner TI, Usdin TB. 1994. Functional identification of a vesicular acetylcholine transporter and its expression from a "cholinergic" gene locus. J Biol Chem 269:21929–21932.

Gilmor ML, Counts GS, Wiley RG, Levey AI. 1998. Coordinate expression of the vesicular acetylcholine transporter and choline acetyltransferase following septohippocampal pathway lesions. J Neurochem 71:2411–2420.

Hicks BW, Rogers GA, Parsons SM. 1991. Purification and characterization of a nonvesicular vesamicol-binding protein from electric organ and demonstration of a related protein in mammalian brain. J Neurochem 57:509–519.

Huttner WB, Schiebler W, Greengard P, De Camilli P. 1983. Synapsin I (protein I), a nerve terminal-specific phosphoprotein. III. Its association with synaptic vesicles studied in a highly purified synaptic vesicle preparation. J Cell Biol 96:1374–1388.

Ichikawa T, Ajiki K, Matsuura J, Misawa H. 1997. Localization of two cholinergic markers, choline acetyltransferase and vesicular acetylcholine transporter in the central nervous system of the rat: in situ hybridization histochemistry and immunohistochemistry. J Chem Neuroanat 13:23–39.

Jung Y-W., Van Dort ME, Gildersleeve DL, Wieland DM. 1990. A radiotracer for mapping cholinergic neurons of brain. J Med Chem 33:2065–2068.

Jung Y-W, Frey KA, Mulholland GK, del Rosario R, Sherman PS, Raffel DM, Van Dort ME, Kuhl DE, Gildersleeve DL, Wieland DM. 1996. Vesamicol receptor mapping of brain cholinergic neurons with radioiodine-labeled positional isomers of benzovesamicol. J Med Chem 39:3331–3342.

Kish SJ, Distefano LM, Dozic S, Robitaille Y, Raiput A, Deck JHN, Hornykiewicz O. 1990. [^{3}H]Vesamicol binding in human brain cholinergic deficiency disorders. Neurosci Lett 117:347–352.

Kuhl DE, Minoshima S, Fessler JA, Frey KA, Foster NL, Ficaro EP, Wieland DM, Koeppe RA. 1996. In vivo mapping of cholinergic terminals in normal aging, Alzheimer's disease, and Parkinson's disease. Ann Neurol 40:399–410

Marien MR, Parsons SM, Altar CA. 1987. Quantitative autoradiography of brain binding sites for the vesicular acetylcholine transport blocker 2-(4-phenylpiperidino) cyclohexanol (AH5183). Proc Natl Acad Sci USA 84:876–880.

Matsumoto RR, Bowen WD, Tom MA, NhiVo V, Truong DD, De Costa BR. 1995. Characterization of two novel σ receptor ligands: antidystonic effects in rats suggest σ receptor antagonism. Eur J Pharmacol 280:301–310

McCann DJ, Su T-P. 1990. Haloperidol-sensitive (+)[^{3}H]SKF-10,047 binding sites (σ sites) exhibit a unique distribution in rat brain subcellular fractions. Eur J Pharmacol 188:211–218.

McCann DJ, Rabin RA, Rens-Domiano S, Winter JC. 1989. Phencyclidine/SKF-10,047 binding sites: evaluation of function. Pharmacol Biochem Behav 32:87–94.

Meyer EM, Bryant SO, Wang R-HD, Watson RJ. 1993. Characterization of [^{3}H]vesamicol in rat brain preparations. Neurochem Res 18:1067–1072.

Mulholland GK, Jung Y-W. 1992. Improved synthesis of [^{11}C]methylaminobenzovesamicol. J Labelled Comp Radiopharm 31:253–259.

Mulholland GK, Jung Y-W, Wielamd DM, Kilbourn MR, Kuhl DE. 1993. Synthesis of [^{18}F]fluoroethoxy-benzovesamicol, a radiotracer for cholinergic neurons. J Labelled Comp Radiopharm 33:583–591.

Perry EK. 1980. The cholinergic system in old age and Alzheimer's disease. Age Ageing 9:1–8.

Perry EK, Tomlinson BE, Blessed G, Bergmann K, Gilson PH, Perry RH. 1978. Correlation of cholinergic abnormalities with senile plaques and mental test scores in senile dementia. Br Med J 2:1457–1459.

Rogers GA, Parsons SM, Anderson DC, Nilsson LM, Bahr BA, Kornreich WD, Kaufman R, Jacobs RS, Kirtman B. 1989. Synthesis, in vitro acetylcholine-storage-blocking activities, and biological properties of derivatives and analogues of trans-2-(4-phenylpiperidino)-cyclohexanol (vesamicol). J Med Chem 32:1217–1230.

Rogers GA, Kornreich WD, Hand K, Parsons SM. 1993. Kinetic and equilibrium characterization of vesamicol receptor ligand complexes with picomolar dissociation constants. Mol Pharmacol 44: 633–641.

Roghani A, Feldman J, Kohan SA, Shirzadi A, Gundersen CB, Brecha N, Edwards RH. 1994. Molecular cloning of a putative vesicular transporter for acetylcholine. Proc Natl Acad Sci USA 91:10620–10624.

Ruberg M, Mayo W, Brice A, Duyckaerts C, Hauw JJ, Simon H, LeMoal M, Agid Y. 1990. Choline acetyltransferase activity and [^{3}H]vesamicol binding in the temporal cortex of patients with Alzheimer's disease, Parkinson's disease, and rats with basal forebrain lesions. Neuroscience 35:327–333.

Usdin TB, Eiden LE, Bonner TI, Erikson JD. 1995. Molecular biology of vesicular ACh transporter. Trends Neurosci 18:218–224.

Van Dort ME, Jung Y-W, Gildersleeve DL, Hagen CA, Kuhl DE, Wieland DM. 1993. Synthesis of the ^{123}I- and ^{125}I-labeled cholinergic nerve marker (-)-5-iodobenzovesamicol. Nucl Med Biol 20: 929–937

Varoqui H, Diebler M-F, Meunier F-M, Rand JB, Usdin TB, Bonner TI, Eiden LE, Erickson JD. 1994. Cloning and expression of the vesamicol binding protein from the marine ray Torpedo. FEBS Lett 342:97–102.

Wilcock GK, Esiri MM, Bowen DM, Smith CCT. 1982. Alzheimer's disease: correlation of cortical choline acetyltransferase activity with the severity of dementia and histological abnormalities. J Neurol Sci 57:407–417.

Whittaker VP, Michaelson IA, Kirkland RJA. 1964. The separation of synaptic vesicles from nerve-ending particles ('synaptosomes'). Biochem J 90:293–303.